

Influence of transition metals (Sc, Ti, V, Cr, and Mn) doping on magnetism of CdS

Zhongqiang Suo(索忠强), Jianfeng Dai(戴剑锋), Shanshan Gao(高姗姗), Haoran Gao(高浩然)

Citation: Chin. Phys. B . 2020, 29(11): 117502 . **doi:** 10.1088/1674-1056/aba2e6
Journal homepage: http://cpb.iphy.ac.cn; http://iopscience.iop.org/cpb

What follows is a list of articles you may be interested in

Microstructure and ferromagnetism ofheavily Mn doped SiGe thin flims

Huanming Wang(王焕明), Sen Sun(孙森), Jiayin Xu(徐家胤), Xiaowei Lv(吕晓伟), Yuan Wang(汪渊), Yong Peng(彭勇), Xi Zhang(张析), Gang Xiang(向钢)

Chin. Phys. B . 2020, 29(5): 057504 . **doi:** 10.1088/1674-1056/ab8219

Two-dimensional XSe_2 (X=Mn, V) based magnetic tunneling junctions with high Curie temperature

Longfei Pan(潘龙飞), Hongyu Wen(文宏玉), Le Huang(黄乐), Long Chen(陈龙), Hui-Xiong Deng(邓惠雄), Jian-Bai Xia(夏建白), Zhongming Wei(魏钟鸣)

Chin. Phys. B . 2019, 28(10): 107504 . **doi:** 10.1088/1674-1056/ab3e45

Magnetism induced by Mn atom doping in SnO monolayer

Ruilin Han(韩瑞林), Yu Yan(闫羽)

Chin. Phys. B . 2018, 27(11): 117505 . **doi:** 10.1088/1674-1056/27/11/117505

Ferromagnetism and magnetostructural coupling in V-doped MnNiGe alloys

Hui Yang(杨慧), Jun Liu(刘俊), Chao Li(李超), Guang-Long Wang(王广龙), Yuan-Yuan Gong(龚元元), Feng Xu(徐锋)

Chin. Phys. B . 2018, 27(10): 107502 . **doi:** 10.1088/1674-1056/27/10/107502

Half-metallic ferromagnetism in C-doped zinc-blende ZnO: A first-principles study

Dan Xu, Yao Kai-Lun, Gao Guo-Ying, Ma Guo-Qiang

Chin. Phys. B . 2013, 22(4): 047507 . **doi:** 10.1088/1674-1056/22/4/047507

Influence of transition metals (Sc, Ti, V, Cr, and Mn) doping on magnetism of CdS*

Zhongqiang Suo(索忠强)[1], Jianfeng Dai(戴剑锋)[1,2,†], Shanshan Gao(高姗姗)[1], and Haoran Gao(高浩然)[1]

[1] School of Science, Lanzhou University of Technology, Lanzhou 730050, China
[2] State Key Laboratory of Advanced Processing and Recycling of Nanoferrous Metals, Lanzhou 730050, China

(Received 13 May 2020; revised manuscript received 2 July 2020; accepted manuscript online 6 July 2020)

The influence of transition metals (Sc, Ti, V, Cr, and Mn) doping at different distances on the magnetism of CdS is studied by using generalized gradient approximation combined with Hubbard U in the VASP package. The results show that the doping systems are more stable, easy to form, and the wurtzite structure of CdS is not changed. It is found that the systems are antiferromagnetic (AFM) when nearest neighbor doping, which is attributed to the direct charge transfers between two impurity ions. The systems are ferromagnetic (FM) when the doping distance increases further, since the double exchange interactions are observed among the 3d orbital of the transition metal, the Cd-5s and the S-3p orbitals are at conduction band minimum. We also found that the total magnetic moment of each ferromagnetic system increases with the order of SC to Mn-doping, the spin polarizability of Cr-doping system is 100%. The estimated Curie temperature indicates that the Cr- and Mn-doped CdS in this paper can achieve room-temperature ferromagnetic characteristics, especially the Cr doping is the most prominent. And TM-doping does not destroy the semiconductor characteristics of the system. Therefore, the TM-doped CdS can be used as an ideal dilute magnetic semiconductor functional material.

Keywords: transition metals doping, electronic structure, magnetism, CdS, Curie temperature

PACS: 75.50.Pp, 75.50.Cc, 71.20.–b, 71.15.Mb **DOI:** 10.1088/1674-1056/aba2e6

1. Introduction

The motivation of diluted magnetic semiconductors (DMS) is to find new materials and technologies to create devices with new functions. At present, the DMSs with room-temperature ferromagnetism have attracted considerable attention for possible applications in spintronics. As one of the important carriers in DMS, CdS has a band-gap of 2.42 eV at room temperature, known for its comparatively low resistivity, high photoconductivity,[1] large absorption coefficient, and high refractive index (between 2.5 and 2.7) in the visible range.[2,3] Due to its special properties, it is used in areas such as ultra-sensitive magnetic field sensors, electro–optic switches,[4] magneto–optical,[5] quantum-based logic, and memory devices for high-speed computations,[6] *etc*.

An ideal DMS should have ferromagnetic (FM) characteristics at or above room temperature. Generally, the magnetic properties of the material is controlled by changing the composition of the magnetic particles in the DMS. For example, Kim[7] observed Mn and Zn co-doped CdS single crystal nanowires, which exhibited room-temperature FM behavior. Bogle[8] synthesized CdS:Co nanoparticles, weak magnetism is realized, and it decreases at higher cobalt concentration. Sanjeev[9] reported that the magnetic behavior has been shown by CdS nanoparticles doped with Ni (3%) and CdS nanoparticles co-doped with Ni (3%) and Cu. In Ref. [10], Murali *et al*. reported that the room-temperature ferromagnetism has been observed in Fe-doped CdS nanocrystals. Murali *et al*.[11] synthesized the CdS:Mn nanowires and obtained significant room-temperature ferromagnetism, and the ferromagnetism is enhanced with the increase of Mn^{2+} concentration. Zhao *et al*.[12] found that as-prepared CdS:Eu nanoparticles exhibited distinct and stronger room-temperature ferromagnetism. Elavarthi *et al*.[13] indicated that the diamagnetic CdS nanoparticles are transformed to FM for 3% Cr^{3+} doping by VSM studies. Wang *et al*.[14] synthesized a wurtzite CdS:Y nanocrystal with room-temperature ferromagnetism via an effective doping atomization method. Anbarasi *et al*.[15] reported that super-paramagnetic and FM orderings were observed for the Sr-doped CdS films. Samiyammal *et al*.[16] synthesized Ba-doped CdS films and found that the doped films have FM characteristics. Altaf's finding[17] showed that H added on the Cd-top site makes it FM and half-metallic above the room temperature.

In summary, most DMSs are prepared by using CdS as the main component and transition metals (TM) as dopant.[7–12] TM-doping makes it multifunctional to achieve the desired properties.[18] However, the experimental results cannot analyze the root cause of magnetic properties of materials from the electronic level, the magnetic source is controversial. Many experiments are doped with TM single-doping, the object of the study is not systematic, the regularity is not obvi-

*Project supported by the National Natural Science Foundation of China (Grant No. 11664023) and the HongLiu First-class Disciplines Development Program of Lanzhou University of Technology and State Key Laboratory of Advanced Processing and Recycling of Nonferrous Metals of China.

†Corresponding author. E-mail: daijf@lut.cn

© 2020 Chinese Physical Society and IOP Publishing Ltd

ous, and it is difficult to control the position and distance of the doping in the experiment. Therefore, the magnetic properties of TM-doped (Sc-, Ti-, V-, Cr-, Mn-doped) CdS are systematically studied based on the density functional theory. This paper mainly studied influence of atomic number and doping distance on structural characteristics and magnetic properties, analyzed the micro-mechanism and experimental results, provided theoretical guidance for experiments. So, it is meaningful to study the TM-doped CdS based on density functional theory.

2. Computational details

2.1. Theoretical models

The CdS of wurtzite structure belongs to the $P63$ mc space point group, and its unit cell is formed by the hexagonal close row of Cd and the hexagonal close row of S in the c-axis direction.[4] Normally, the lattice constants of CdS are $a = b = 4.135$ Å, $c = 6.749$ Å, $c/a = 1.632$, $\alpha = \beta = 90°$, $\gamma = 120°$. Based on the wurtzite CdS cells, twenty-one supercells ($2 \times 2 \times 2$) are established. Pure CdS is shown in Fig. 1(a). Figure 1(b) is the two same TM nearest-neighbor dopings, the distance (atomic center) between the doping atoms is about 4.49 Å; figure 1(c) is the two same TM next nearest-neighbor dopings, the distances is about 5.00 Å. The distance between the doping atoms of Figs. 1(d) and 1(e) are 5.34 Å and 7.07 Å, respectively. The five TMs (Sc, Ti, V, Cr, and Mn) are doped as described above. Doping systems of Figs. 1(b)–1(e) are denoted by TM_1, TM_2, TM_3, and TM_4, respectively.

2.2. Calculation method

The calculations are performed using VASP 5.4.4 package based on spin polarization density functional theory. The functional of exchange–correlation effect is treated using the Perdew–Burke–Ernzerhof version of the generalized gradient approximation (GGA). The traditional method of GGA is usually only about 25% of the experimental value for the excited state of a multi-particle system, and the calculated properties are inaccurate due to the self-interaction of GGA algorithm. Thus, using Hubbard U to correct the band-gap (GGA $+U$) in this article.

The formal charges of the Sc, Ti, V, Cr, and Mn atoms in this paper are +3, +2, +2, +2, and +2, respectively. The electronic configurations[19] of the ions used for the calculation are Sc-$3s^2 3p^6$, Ti-$3d^2$, V-$3d^3$, Cr-$3d^4$, Mn-$3d^5$, Cd-$4d^{10}$, and S-$3s^2 3p^6$, the plane cut-off energy in inverted space $E_{cut} = 400$ eV, the K-points in the Brillouin zone is set to $4 \times 4 \times 2$. First, we optimize the FM and AFM structures of each system, the initial magnetic moment is 3 μ_B, the optimization ends when the total energy of the system is less than 10^{-5} eV/atom and the force of each atom is less than 10^{-2} eV/Å. Then, the self-consistent field is calculated using the same convergence accuracy as relaxation. Finally, the property of magnetism related is calculated.

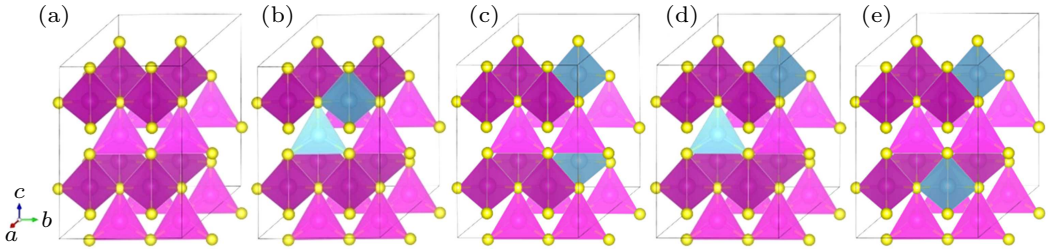


Fig. 1. Supercell ($2 \times 2 \times 2$) model of pure (a) and doped CdS [(b)–(e)]. Magenta, cyan, and yellow are Cd, doping atoms, and S, respectively.

3. Results and discussion

3.1. Structural characteristics

In order to explore the feasibility and reliability of the doping, it is necessary to perform atomic relaxation and electronic self-consistency for each system, and calculate the lattice constant and formation energy. By performing calculations, we obtained the most stable structure, the parameters of pure-CdS are $a = 4.186$ Å and $b = 6.841$ Å, which are very close to the experimental values ($a = 4.149$ Å, $c = 6.779$ Å),[20] the errors are only 0.89% and 0.91%, respectively. The axial ratio (c/a) of pure-CdS is 1.634, which is quite similar to the experimental value (1.63),[20] and the c/a of each doping system is 1.611 ± 0.01, indicating that the lattice calculated has not been distorted and the results are reliable, the doping models are reasonable. Figure 2 is the volume change diagram of each system. The results show that the TM-doping makes the volume of each doping system slightly decreasing, which is closely related to the radius of the TM atom. The radius of Sc atom is the smallest (Cd^{2+} 0.95 Å > Ti^{2+} 0.90 Å > V^{2+} 0.88 Å > Cr^{2+} 0.84 Å > Mn^{2+} 0.83 Å > Sc^{3+} 0.81 Å),[4,21,22] but the volume is the largest in the doping system. The reason is that the volume expansion[23] due to the repulsion between the extra positive charges after Sc^{3+} replaces Cd^{2+}, which leads to the energy increase of the system. The volumes of other TMs (Ti, V, Cr, and Mn) are decreased with the increase of the atomic number, which is consistent with the change of the radius of the doping atom. Further analysis shows that the volumes of the Sc-doping system are decreased with the distance increases between the two

Scs. The reason may be that the repulsion between positive charges is decreased with the distance increases between the doping atoms. In the other four kinds of TM systems, the system volumes of all the nearest-neighbor dopings are the smallest.

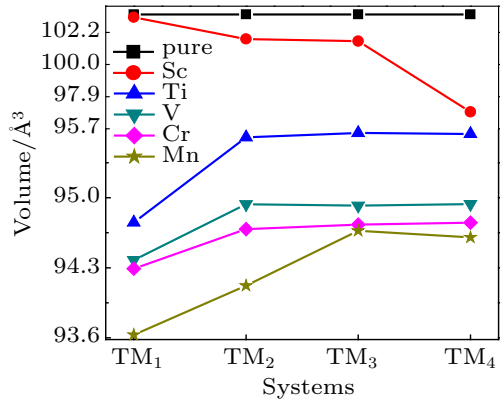


Fig. 2. The volumes of each system after structural optimizations.

The formation energies (E_F) of each system are shown in Fig. 3. It is clear from Fig. 3 that the E_F of each TM-doping system are negative, and lower than that of the pure-CdS. This indicates that the doping is feasible and the doping systems are easy to form. It is also easy to form Cr- or Mn-doped CdS in experiments,[24,25] this shows that the calculated results in this paper are reliable. Further analysis shows that the stability of each TM system weakens with the order of Ti, V, Cr, Mn, and Sc.

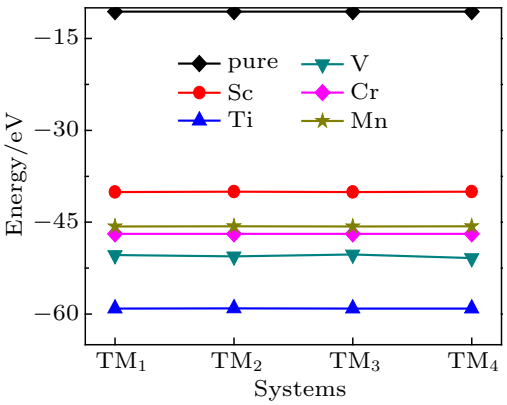


Fig. 3. The E_F of each doping system.

The E_F of each system can be calculated as follows:[4]

$$E_F = E_d - E_p - 2\mu_{TM} + 2\mu_{cd}, \quad (1)$$

where E_d and E_p are the total energies of the doping system and the pure-CdS, respectively. The μ_{TM} and $2\mu_{cd}$ represent the chemical potentials of the doping atom and Cd atom, respectively.

3.2. Magnetic moment

In order to explore the effective part of the sum of various magnetic moments inside the atom, we calculate the total magnetic moment (Mag) of each system and the spin magnetic moment of each atom.

The magnetic moments of each system are shown in Table 1. Where TM1 and TM2 represent the net magnetic moments of the two TM impurity atoms. The results illustrate that the TM (Sc, Ti, V, Cr, and Mn) doping can make CdS magnetic, and the doping distance will affect the Mag of the system. The magnetic moment of Sc_1 and Sc_2 are 0.938 μ_B and 0.891 μ_B, respectively, which is in line with the characteristics of ferromagnetism. Sc_3 and Sc_4 are typical antiferromagnetism. In Ti-, V-, Cr-, and Mn-doping systems, the systems are AFM when TM-dopings are nearest-neighbors, this is due to the direct exchange between two magnetic ions, resulting in a local net magnetic moment near the Fermi level (E_f) is 0 μ_B. The systems are FM when the doping distance between the impurity ions increases slightly, because the local net spins are generated between TM1 and TM2, this results in the system having Mag. The above analysis verifies the literature[26] that "the direct exchange between Mn^{2+} in the bulk is typically AFM". The reason for nature of the Sc system being not very similar to other TMs is the special formal charge of the Sc atom. In Subsection 3.4, we will further confirm the uniqueness of the Sc-doping. Anyway, when Sc, Ti, V, Cr, and Mn-dopings happened, the magnetic moments of each TM-system are approximately 1, 4, 6, 8 and 10 μ_B, respectively. It illustrates that the magnetic moment increases with the increase of the atomic number of TM (order of Sc to Mn), but the doping distance has no significant effect on the Mag of each FM system.

Table 1. The magnetic moment of each system and net magnetic moment of the TM atom. The minus sign denotes spin-down.

Structure	Mag/μ_B	TM1/μ_B	TM2/μ_B
Sc_1	0.938	0.301	0.272
Sc_2	0.891	0.257	0.257
Sc_3	0	0.160	−0.159
Sc_4	0	0.216	−0.216
Ti_1	0	1.238	1.239
Ti_2	−3.989	1.466	1.466
Ti_3	3.996	1.492	1.482
Ti_4	3.987	1.487	1.487
V_1	0	2.436	−2.437
V_2	5.950	2.410	2.410
V_3	5.949	2.427	2.416
V_4	5.859	2.443	2.443
Cr_1	0	3.442	−3.442
Cr_2	8.004	3.478	3.479
Cr_3	7.996	3.485	3.465
Cr_4	7.999	3.489	3.487
Mn_1	0	4.190	−4.189
Mn_2	10.000	4.157	4.227
Mn_3	9.998	4.166	4.164
Mn_4	9.912	4.174	4.174

3.3. Magnetic source

In the following description, we use the partial electron density and differential charge density distribution to illustrate the source of magnetics. The former visually indicates the distribution of electrons and the nature of chemical bonds among orbitals at the electronic level. The latter can clearly analyze the interface bonding type and phenomenon of charge transfer. Only the partial electron density ((010) and (100)) at conduction band minimum (CBM) and the differential charge density (100) are shown in Fig. 4, since the systems in this article are all N-type semiconductors, the doping mainly affects the conduction band (CB). Considering that Ti-doping systems are the most stable, it is reasonable to select Ti system as the research object. In the pure CdS, the valence band maximum (VBM) is composed mainly of S-3p non-bonding states, while the CBM is dominated by the Cd-4d non-bonding states as shown in Fig. 4(a). Ti–S and Ti–Ti bondings are shown in Fig. 4(b), which is substantially different from the non-bonding states of Cd-4d in Fig. 4(a). The orbital hybridization is observed at the VBM of Ti-doping CdS. As depicted by Figs. 4(b)–4(e), the doping distance has not changed the type of the bond.

From the differential charge density in Fig. 4(b), it can be seen the phenomenon of direct charge transfer between Ti and Ti under the action of the newly formed Ti–S bond in the Ti nearest-neighbor doping system. The charge distribution of other particles in the system is similar to the pure CdS (Fig. 4(a)), there is no net magnetic moment generated in the system. This is identical with the analyses in Subsection 3.2. The common feature of the difference diagrams in Figs. 4(c)– 4(e) is that the electrons around it are reduced after Ti-doping, the surrounding charges are concentrated to nearby S and Cd atoms, and there is almost no direct electron transfer between Ti and Ti, which causes the spin electron cloud around Ti atoms to be unevenly distributed, spin-up and spin-down are asymmetric, so local net spins appear at the E_f, the system is magnetic. The analysis of the charge differential density is consistent with the results of the magnetic moment calculations. it is consistent with the theoretical interpretation of the double exchange effect of carriers as the medium.

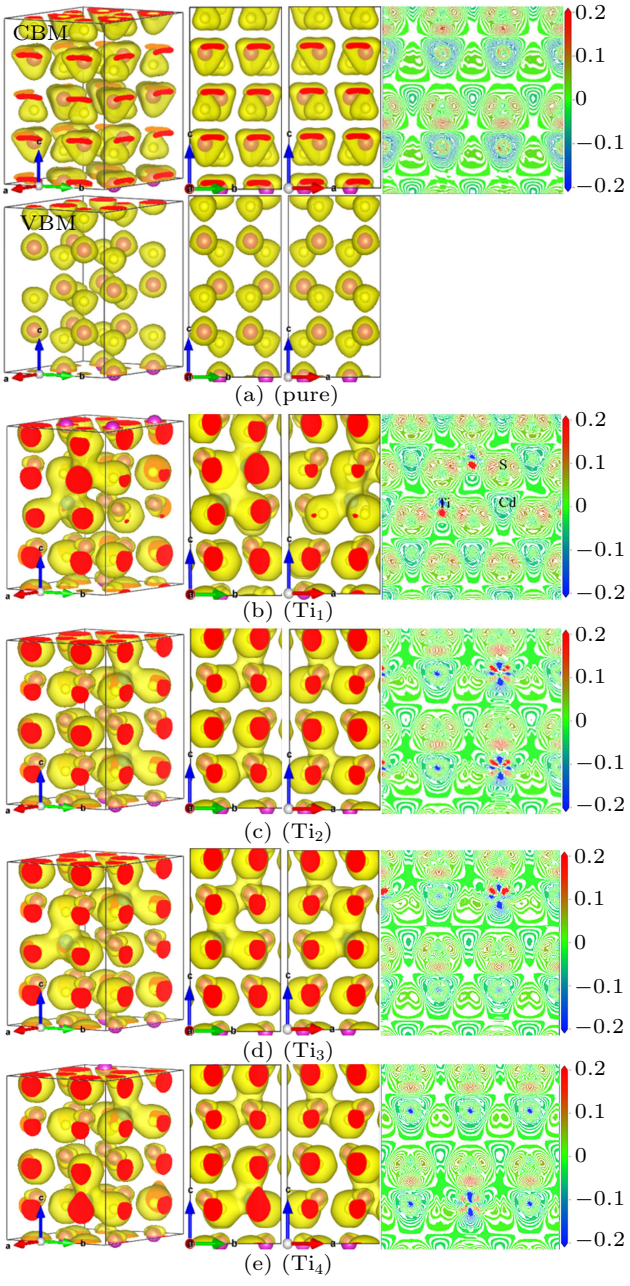


Fig. 4. The partial electron density at CBM and the charge density differential distribution: (a) pure, (b) Ti_1, (c) Ti_2, (d) Ti_3, and (e) Ti_4.

3.4. Magnetic mechanism

In order to explore the magnetic mechanism, it is necessary to analyze the electronic components of each system. Figure 5 shows clearly that the valence band (VB) of each system is mainly composed of S-3p, followed by Cd-4d, TM-3d, and few Cd-5s, the CB is mainly composed of TM-3d, followed by S-3p, S-3s, and a small amount of Cd-4d. As shown in Fig. 5, the change of the atom doping distance has little effect on the electronic structure of the system (taking Ti atom as an example), while the increase of the atomic number has a greater effect on the electronic structure of the system (taking the nearest neighbor doping of each atom as an example).

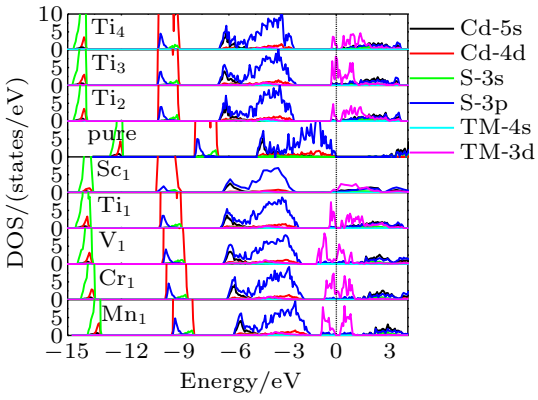


Fig. 5. The partial density of states (PDOS) for each system.

The VBM of each system gradually moved up (high energy region) with the doping order of Sc–Ti, the CBM is occupied by the TM-3d state, and the E_f moved up. Changing the doping distance does not affect the electronic configuration of the system. It is very important for the formation of ferromagnetism for bonding interaction among atoms when crystals are formed. The electron clouds overlap mutually and the electrons exchange with each other when atoms are close to each other to form a molecule. For TM, the energy of the 3d state approaches to 4s electrons, so their electron clouds also overlap in the atom, causing redistributions of s and d electrons. The exchange energy generated by this exchange may align the spin magnetic moments in the same direction, this spin magnetic moment is counter-balanced magnetic moment of the end of d-layer in adjacent atoms. Quantum mechanical calculations indicate that the magnetic moments of adjacent atoms will be parallel arrangement in the same direction when the electron exchange integrals of adjacent atoms inside the magnetic material are positive, thereby achieving spontaneous magnetization.

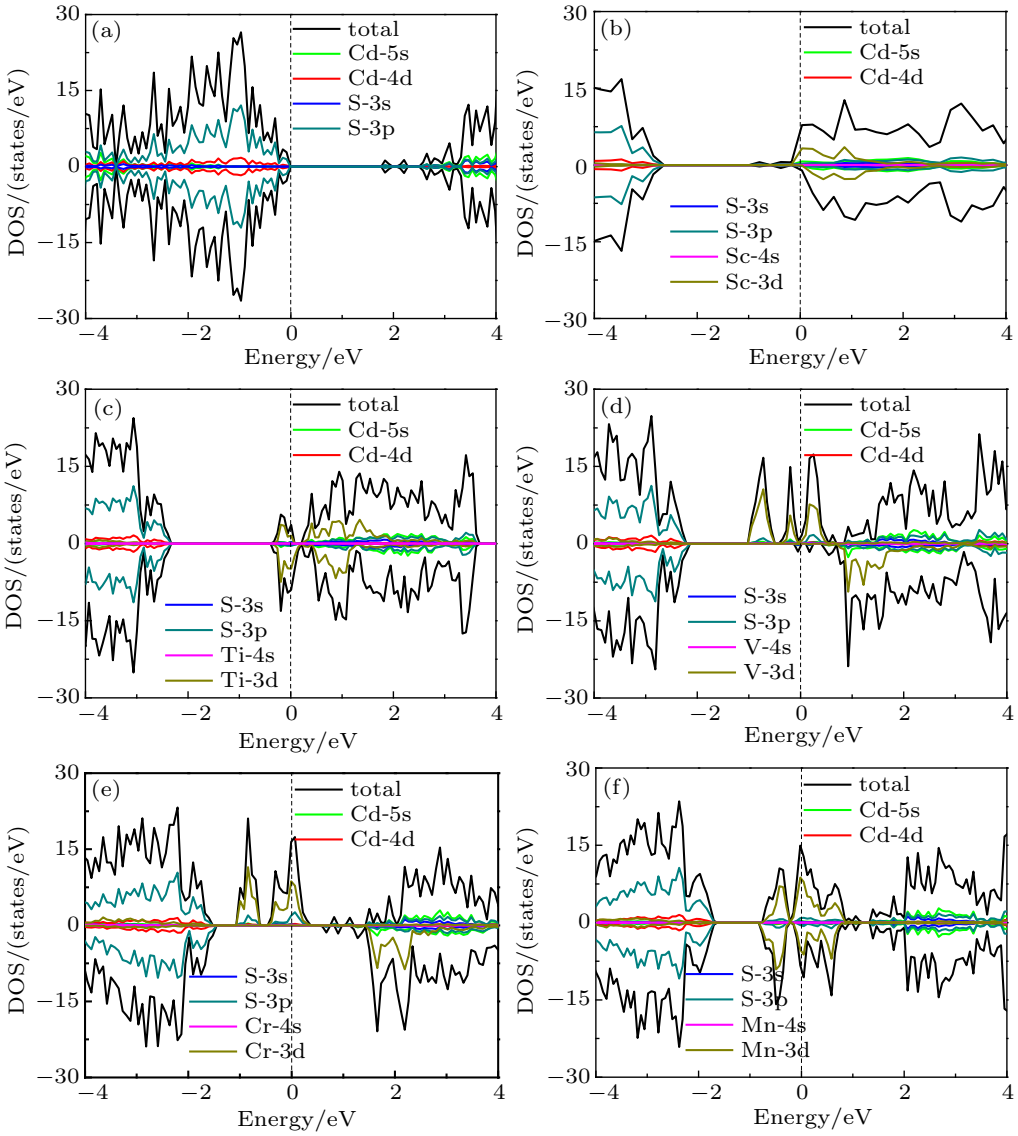


Fig. 6. The total density of states (TDOS) and PDOS of the pure (a), Sc_2 (b), Ti_2 (c), V_2 (d), Cr_2 (e), and Mn_2 (f) structures.

The spin density of states is a good illustration of the magnetic mechanism of the system, as shown in Fig. 6. The results show that the electronic states of all the spins-up and spin-down in the pure CdS are completely symmetrical, the net magnetic moments cancel each other, so the system is non-magnetic. The next nearest-neighbor dopings in all TM systems are FM and the effects of the doping distance on the density of states (DOS) of the FM systems are relatively small, so figures 6(b)–6(f) show the spin state densities of Sc_2, Ti_2, V_2, Cr_2, and Mn_2, respectively. The Sc-doping is shown in Fig. 6(b), which mainly introduces Sc-3d state electrons into the CB. There are electron exchange effects among Sc-3d, Cd-5s, and S-3p orbits in the CBM. The exchange effect leads to the spin-up more than spin-down in the Sc-3d state near the E_f. This spin asymmetry produces the local net magnetic moment, which in turn makes the system magnetic. The DOS curves of

the other four TM-doping systems (Figs. 6(c)–6(f)) are similar. The 3d electrons are introduced into the CBM of CdS when Ti, V, Cr, and Mn are dopings. This moment, the strong electron exchange occurs among TM-3d, Cd-5s, and the S-3p orbitals. Namely, double exchange interactions, which make the net spin appears at E_f, the system has Mag. In short, the reason why TM-doping makes the system magnetic is that the doping makes the electron spin-up and spin-down at E_f asymmetric. The above analysis is consistent with the exchange effect in Subsection 3.3. It is consistent with the theoretical interpretation of the double exchange effect of carriers as the medium.[27,28] It is shown from Fig. 6(c) that, the electron state of the upward spin at the E_f is less than the downward, so the Mag of Ti_2 is downward, this is compliance with the calculation of the magnetic moment.

In addition, for the integrity of Fig. 5, the deep full bands of Sc-doping are not represented. The deep energy levels of Ti, V, Cr, and Mn are all around −14 eV, but the Sc-systems are −50 eV. The overall analysis of Fig. 6 shows that figure 6(b) is different from other systems in that its state density curve is relatively flat, this indicates that its energy band is wide, the band curve is sharp, the delocalization is strong, and the effective mass is small.[29] Therefore, it is not surprising that the properties of the Sc-doping are slightly different from those of the other four TM-dopings, this also validates the analysis in Subsection 3.2.

According to the definition of the spin polarizability (P), it is known that the spin polarizability of the system in the V-doping and Cr-doping is 100%. $P = (N\uparrow - N\downarrow)/(N\uparrow + N\downarrow)$, where $N\uparrow$ and $N\downarrow$ are the majority and minority density carriers. Hence, the TM-doped CdS in this paper can be used as an ideal DMS semiconductor functional material. The band diagrams of the spin-up and spin-down of the system can also verify this result.

Figure 7(a) shows the band structure of the pure CdS. The upward and downward spins are symmetrical, so the system is non-magnetic. Its band-gap is 2.417 eV, which is in agreement with the experimental value 2.42 eV,[30] this indicates that the calculations in this paper are reliable. Figures 7(b)–7(f) show the band structures of Sc_2, Ti_2, V_2, Cr_2, and Mn_2, respectively. It can be seen that there is band-gap width in the band structure whether spin-up or spin-down, which indicates that the TM-doping has not destroyed the semiconductor properties of each system. The energy level distributions of spin-up and spin-down are not coincident, scilicet, there are different occupation numbers for spin-up and spin-down states, so the system exhibits magnetism. Further analysis shows that the band structure curve of the Sc-doping system near the E_f is smoother than that of other systems, which further confirms the reliability of the state density analysis. Another main reason for the ferromagnetism is the atomic magnetic moment, and the electron spin magnetic moment plays a major role in the atomic magnetic moment. There are states in which the electron shell of the atom is not filled with electrons in the doping system, which is an important condition for generating ferromagnetism.

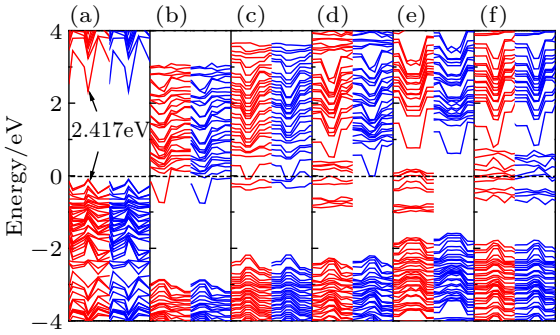


Fig. 7. Energy band structures of pure (a), Sc_2 (b), Ti_2 (c), V_2 (d), Cr_2 (e), and Mn_2 (f) structures. Red and blue indicates spin-up and spin-down, respectively.

3.5. Coupling characteristics and Curie temperature

As we all know, the atomic distance in the crystal lattice increases when the temperature of the system increases, which reduces the exchange coupling effect. At the same time, the thermal motion constantly destroys the regular orientation of the atomic magnetic moment, resulting in the spontaneous magnetization (M_s) decreases. Until the temperature is higher than the Curie point, the original regular magnetic moment orientation in the system is completely destroyed, the magnetic moment of the system no longer exists, and the material changes from FM to paramagnetic. Therefore, it is necessary to analyze the Curie temperature (T_c) and coupling type (coupling) of the material, as shown in Table 3. The T_c can be estimated[31] by the mean field theory of the Heisenberg model ($T_c k_B = 2\Delta E/3C$), where k_B and C are Boltzmann constant and magnetic impurity concentration, respectively. ΔE is the energy difference between the AFM and FM configurations ($\Delta E = E_{AFM} - E_{FM}$). J_{dd} is the exchange constant from Heisenberg Hamiltonian between the AFM and FM. In Ref. [32], the authors reported that the superexchange interaction between the magnetic moments of S and TM atoms could be estimated by Hamiltonian, $\hat{H} = N\sum_i S_i s_i$. The N, S_i, and s_i are the exchange operator involved, the spin operator of impurities and the local spin operator corresponding to s and p states of S atoms. N_{sd} is the s–d exchange constant between Cd-s, S-s, and TM-d electrons, N_{pd} is the p–d exchange constant between S-p and TM-d states.

It can be seen from the J_{dd}, N_{sd}, and N_{pd} in Table 2, when the transition metals Ti, V, Cr, and Mn in the system are nearest-neighbor dopings, there is no d–d exchange and s–d, s–p super-exchanges in the system, the direct exchange between them predominates, which makes the system more inclined to AFM. The direct exchange between TM ions is

weakened when the distance is increased, the system's superexchange mainly from S (3s and 3p) and TM-3d, and the resulting magnetic tends to FM. The effect of the distance between Mn atoms on the magnetic properties of the system is consistent with Ref. [33]. Compared with p–d exchange, the s–p exchange in each system is the dominant position in the double superexchange, which is consistent with the magnetic mechanism analysis in Subsection 3.4. The coupling type of each system is consistent with the magnetic moment analysis, which further verifies the reliability of the magnetic moment calculation. According to the Curie temperature, TM-doped CdS can achieve room-temperature FM characteristics, and Cd doping is most beneficial to DMS at room temperature. The Curie temperature of the Mn-doping is consistent with experiment[11] that of "Mn-doped CdS with ferromagnetism much higher than room temperature". In experiment,[13] all the doped samples (CdS:Cr) exhibited room-temperature ferromagnetism. This further confirms the reliability of the results of this paper, and the estimated values may have errors, but it does not affect the guiding significance.

Table 2. Magnetic performance-related parameters. The star $*$ means more than 1000.

System	J_{dd}/meV	N_{sd}/eV	N_{pd}/eV	ΔE/meV	Coupling	T_c/K
Sc_1	21.16	0.78	0.11	38.47	FM	297
Sc_2	2.61	0.64	0.21	4.39	FM	34
Sc_3	–	–	–	−7.47	AFM	–
Sc_4	–	–	–	−17.22	AFM	–
Ti_1	–	–	–	−4.18	AFM	–
Ti_2	1.03	0.18	0.06	10.58	FM	81
Ti_3	0.62	0.21	0.05	12.28	FM	95
Ti_4	3.07	0.11	0.06	61.10	FM	472
V_1	–	–	–	−30.46	AFM	–
V_2	0.01	2.82	0.18	0.09	FM	1
V_3	0.02	2.81	0.10	0.70	FM	5
V_4	0.01	2.84	0.21	0.18	FM	2
Cr_1	–	–	–	0.10	AFM	–
Cr_2	5.17	2.30	1.96	372.78	FM	$*$
Cr_3	6.34	3.73	0.14	455.96	FM	$*$
Cr_4	6.49	3.78	0.27	467.02	FM	$*$
Mn_1	–	–	–	50.35	AFM	–
Mn_2	0.74	0.10	0.01	81.01	FM	627
Mn_3	0.94	0.38	0.09	103.18	FM	798
Mn_4	0.47	0.02	0.01	50.56	FM	391

4. Conclusions

In short, the structure and magnetic properties of TM-(Sc-, Ti-, V-, Cr-, and Mn-)doped CdS are studied in this paper through the GGA + U method in the VASP package. The structural characteristics show that various doping does not destroy the original lattice structure of CdS, and the doping system is easy to be formed. The magnetic properties are mainly studied through four aspects: magnetic moment calculation, magnetic source analysis, mechanism exploration, and estimation of Curie temperature. The results show that the magnetic moment gradually increases with the sequence of Sc to Mn-doping, the doping distance can determine whether the system is magnetic or not. The spin electron clouds around the impurity atoms are unevenly distributed when TM is doping, which makes the electrons spins asymmetric at the E_f, this leads to the appearance of the local net spin at the CBM, so the system is magnetic. Further analysis shows that this net spin is mainly caused from the electron exchange between the TM-3d orbit of CBM, the Cd-5s orbit, and the S-3p orbit. Finally, we find by estimating the Curie temperature that TM-doping can achieve room-temperature FM characteristics, which shows that the TM-doped CdS can be used as an ideal DMS semiconductor functional material, and Cr- and Mn-dopings are the most prominent. This article analyzes the magnetic characteristics of each doping material from the microstructure, which will provide theoretical basis and guidance for the application of CdS in DMS.

References

[1] Boudjelal M, Belfedal A and Bouadjemi B 2019 *Chin. J. Phys.* **61** 155
[2] Kamran M A Liu R and Shi L J 2013 *J. Phys. Chem. C* **117** 17777
[3] Reddy Y D, Reddy B K and Reddy D S 2008 *Spectroc. Acta Pt. A-Molec. Biomolec. Spectr.* **70** 934
[4] Suo Z and Dai J 2019 *Results Phys.* **15** 102801
[5] Nabi A 2016 *Comput. Mater. Sci.* **112** 210
[6] Awschalom D D and Kawakami R K 2000 *Nature* **408** 923
[7] Kim D S Cho Y J and Park J 2007 *J. Phys. Chem. C* **111** 10861
[8] Bogle K A, Ghosh S and Dhole S D 2008 *Chem. Mat.* **20** 440
[9] Kumar S Kumar S and Jain S 2012 *Appl. Nanosci.* **2** 127
[10] Murali G, Reddy D A and Prakash B P 2012 *Physica B* **407** 2084
[11] Murali G, Reddy D A and Giribabu G 2013 *J. Alloys Compd.* **581** 849
[12] Zhao R, Wang P and Yang T 2015 *J. Phys. Chem. C* **119** 28679
[13] Elavarthi P Kumar A A and Murali G 2016 *J. Alloys Compd.* **656** 510
[14] Wang P, Zhao R and Li Z 2016 *Crystengcomm* **18** 2607
[15] Anbarasi M, Nagarethinam V S and Usharani K 2017 *J. Mater. Sci.-Mater. Electron.* **28** 14848
[16] Samiyammal P, Parasuraman K and Prabh D 2017 *Surf. Eng.* **33** 835
[17] Rahman A U Ullah H and Jamil A 2019 *Physica B* **570** 209
[18] Saikia D, Jami J and Borah J P 2019 *Physica B* **565** 25
[19] Suo Z, Dai J and Gao S 2020 *Results Phys.* **17** 103058
[20] Heiba Z K Mohamed M B and Mostafa N Y 2019 *Appl. Phys. A-Mater. Sci. Process.* **125** 132
[21] Quintelas C, Rocha Z and Silva B 2009 *Chem. Eng. J.* **149** 319
[22] Paula A T Andrei M V and Kholkin L 2005 *Acta Mater.* **53** 5061
[23] Dai J, Suo Z and Li Z 2019 *Results Phys.* **15** 102649
[24] Wang C, Wang H and Fang Z Y 2009 *J. Alloys Compd* **486** 702
[25] Thambidurai M and Muthukumarasamy N 2012 *J. Mater. Sci.-Mater. Electron.* **23** 618
[26] Freeman J and Watson R E 1961 *Phys. Rev.* **124** 1439
[27] Zener C 1951 *Phys. Rev.* **81** 440
[28] Zener C 1951 *Phys. Rev* **82** 403
[29] Li Y J Yu K M and Chen G B 2020 *J. Alloys Compd.* **822** 153567
[30] Zhang J F, Wageh S and Al-Ghamdi A A 2016 *Appl. Catal. B-Environ.* **192** 101
[31] Sato K, Dederics P H and Yoshida H K 2003 *Europhys. Lett.* **61** 403
[32] Story T, Gaazka R R and Frankel R B 1986 *Phys. Rev. Lett.* **56** 777
[33] Nabi A 2016 *Comput. Mater. Sci.* **112** 210